

## Two and three-dimensional simulation of seawater intrusion: performances of the “SUTRA” and “HST3D” models

F. Ghassemi<sup>1</sup>, T.H. Chen<sup>1</sup>, A.J. Jakeman<sup>1</sup> & G. Jacobson<sup>2</sup>

The problem of seawater intrusion in coastal aquifers and oceanic islands is not a new one and a great deal of research has been undertaken since the late 19th century. The first model was developed in 1888 and is known as the Ghyben–Herzberg. It is a simple model based on the hydrostatic balance between fresh and saline water. With the advent of large computing capacity over the past few decades, more sophisticated models have been developed for the simulation of seawater intrusion and upconing of saline water beneath a pumping well.

Two of the latest developments in this area are the SUTRA and HST3D models. SUTRA is a two dimensional, finite-element, density dependent, solute transport model, while HST3D is a

three-dimensional finite-difference model. This paper describes an application of these two models for the simulation of seawater intrusion in Nauru Island in the Pacific Ocean and it compares their performances. While SUTRA is a powerful model, it cannot adequately simulate three-dimensional problems, because of its two-dimensional nature. On the other hand, HST3D is suitable for the three-dimensional simulation of seawater intrusion, but it requires a small grid size and short time steps. This leads to the solution of a significantly large set of linear equations, necessitating the availability of sophisticated computing facilities in terms of memory and computing power. This makes the use of present-day supercomputers an inevitable requirement.

### Introduction

Many population centres in coastal areas of the world and oceanic islands are dependent on local fresh groundwater resources. However, these resources may be subject to minor or severe seawater intrusion. Countries with this kind of problem include Australia (Hillier, this issue), Belgium, France, Greece, Germany, Indonesia, Iran, Israel, Lebanon, Libya, The Netherlands, Philippines, Spain, Thailand, United Kingdom, and the United States. The list of vulnerable islands is much longer and includes: Bermuda, Canary Islands, Christmas Island (Kiritimati), Cocos (Keeling) Islands, Guam, Hawaiian Islands, Mauritius, Seychelles; and South Pacific Islands including Cook Islands, Ellice Islands, Fiji Islands, Gilbert Islands, Solomon Islands and Tarawa (Falkland, 1991).

The problem of seawater intrusion in coastal aquifers is not new. The first model was developed independently by Ghyben from the Netherlands in 1888 and Herzberg from Germany in 1901. This simple model is known as the Ghyben–Herzberg model and is based on the hydrostatic balance between fresh and saline water in a U-shaped tube (Reilly & Goodman, 1985). This simplistic model ignores convection, dispersion and diffusion phenomena responsible for the distribution of salinity in coastal and island aquifers.

In coastal and island aquifers, freshwater usually overlies the seawater separated by a transition zone. In these cases, management of limited groundwater resources is a delicate problem and requires special attention to minimise the extension of seawater intrusion into aquifers and upconing of seawater near pumping stations. The extent of intrusion depends on a number of factors, including aquifer geometry and properties (hydraulic conductivity, anisotropy, porosity and dispersivity), abstraction rates and depth, recharge rate, and distance of pumping wells from the coastline. Sophisticated tools are required to quantify these factors.

The physical problem is one of density-dependent groundwater flow and solute transport (Voss, 1984; Reilly & Goodman, 1987). Prediction of behaviour can be obtained

by the solution of two partial differential equations describing the “conservation of mass of fluid” and “conservation of mass of salt” in a porous media. Numerical procedures for solving the governing equations require adequate discretisation in space and time as well as appropriate initial and boundary conditions. The set of linear equations generated by spatial discretisation should be solved repeatedly as the simulation time advances. A brief description of the governing equations follows.

### Conservation of mass of fluid

The fluid mass balance in a saturated porous media can be expressed as:

$$\frac{\delta(\epsilon\rho)}{\delta t} = -\nabla \cdot (\epsilon\rho V) + Q_p \quad (1)$$

where  $\epsilon(x,y,t)$  is porosity (dimensionless),  $\rho(x,y,t)$  is fluid density ( $ML^{-3}$ ),  $Q_p(x,y,t)$  is fluid mass source [ $M(L^3T)^{-1}$ ],  $V(x,y,t)$  is average fluid velocity ( $LT^{-1}$ ),  $x$  and  $y$  are coordinate variables (L),  $t$  is time (T), and  $\nabla$  is  $(\delta/\delta x)i + (\delta/\delta y)j$ . This equation can be modified by taking into account two primary dependent variables  $p$  (pressure) and  $C$  (concentration):

$$(\rho S_{op}) \frac{\partial p}{\partial t} + \left( \epsilon \frac{\partial \rho}{\partial C} \right) \frac{\partial C}{\partial t} - \nabla \cdot \left[ \left( \frac{\epsilon \rho k}{\mu} \right) (\nabla p - pg) \right] = Q_p \quad (2)$$

where  $S_{op} = (1-\epsilon)\alpha + \epsilon\beta$  is specific pressure storativity ( $LT^2 M^{-1}$ ),  $\alpha$  is porous matrix compressibility ( $LT^2 M^{-1}$ ),  $\beta$  is fluid compressibility ( $LT^2 M^{-1}$ ),  $C$  is solute concentration as a mass fraction or mass of solute per mass of fluid ( $M_s M^{-1}$ ) which is zero for freshwater and 0.0357 for seawater,  $k(x,y)$  is solid matrix permeability ( $L^2$ ),  $\mu(x,y,t)$  is fluid viscosity [ $M(LT)^{-1}$ ],  $p(x,y,t)$  is fluid pressure [ $M(LT^2)^{-1}$ ], and  $g$  is acceleration due to gravity ( $LT^{-2}$ ).

### Conservation of mass of salt

The solute mass balance for a single species stored in solution is expressed as:

$$\frac{\partial(\epsilon\rho C)}{\partial t} = -\nabla \cdot (\epsilon\rho VC) + \nabla \cdot \{ \epsilon p (D_m I + D) \cdot \nabla C \} + Q_p C^* \quad (3)$$

where  $D_m$  is apparent molecular diffusivity of solutes in

<sup>1</sup> Centre for Resource and Environmental Studies, The Australian National University, GPO Box 4, Canberra ACT, 2601.

<sup>2</sup> Australian Geological Survey Organisation, GPO Box 378, Canberra ACT, 2601.

solution in a porous medium ( $L^2T^{-1}$ ),  $I$  is the identity tensor (dimensionless),  $D$  is the dispersion tensor ( $L^2T^{-1}$ ), and  $C^*$  is the concentration of fluid sources as a mass fraction ( $M_sM^{-1}$ ).

The mechanical dispersion tensor  $D$  is related to the velocity of groundwater flow. For an isotropic porous medium in two spatial dimensions it is expressed as follows:

$$D = \begin{bmatrix} D_{xx} & D_{xy} \\ D_{yx} & D_{yy} \end{bmatrix} \quad (4)$$

The tensor  $D$  is symmetric and its elements are:

$$\begin{aligned} D_{xx} &= \frac{1}{V^2} (d_L V_x^2 + d_T V_y^2) \\ D_{yy} &= \frac{1}{V^2} (d_T V_x^2 + d_L V_y^2) \\ D_{xy} = D_{yx} &= \frac{1}{V^2} (d_L - d_T) (V_x V_y) \end{aligned} \quad (5)$$

where  $V(x,y,t) = (V_x^2 + V_y^2)^{1/2}$  is the magnitude of fluid velocity ( $LT^{-1}$ ),  $V_x(x,y,t)$  and  $V_y(x,y,t)$  are the components of velocity in the  $x$  and  $y$  directions ( $LT^{-1}$ ), and  $d_L(x,y,t)$  and  $d_T(x,y,t)$  are respectively, the longitudinal and transverse dispersion coefficients ( $L^2T^{-1}$ ). The longitudinal and transverse dispersion coefficients cause dispersion along the direction of fluid flow and perpendicular to it. The coefficients  $d_L$  and  $d_T$  are velocity dependent, viz.

$$\begin{aligned} d_L &= \alpha_L V \\ d_T &= \alpha_T V \end{aligned} \quad (6)$$

and  $\alpha_L(x,y)$  and  $\alpha_T(x,y)$  are the longitudinal and transverse dispersivity of the solid matrix ( $L$ ).

‘‘SUTRA’’ and ‘‘HST3D’’ models

A package known as SUTRA (Saturated–Unsaturated TRANsport) was developed by Voss (1984). It employs a two-dimensional finite-element approximation of the governing equations in space, and an implicit finite-difference approximation in time. The method is stable and accurate when employed with proper spatial and temporal discretisation. More recently, another package known as HST3D (Heat and Solute Transport in 3D) has been developed by Kipp (1987). This program employs three-dimensional finite-difference approximations of the governing equations, similar to those presented in the previous section.

The following sections describe the hydrogeological features of Nauru Island and the application of these models for its simulation.

Hydrogeology of Nauru Island

Nauru Island in the Pacific Ocean (Fig. 1) is a raised atoll capping a volcanic seamount rising from an ocean floor depth of 4300 m. The island supports a population of 8500 and occupies a land area of 22 km<sup>2</sup> (Fig. 2) which rises to 70 m above mean sea level (MSL). The island has been mined for its surficial phosphate deposits for about 80 years. About 80% of the land area has had its vegetation and soil cover removed, leaving an exposed limestone

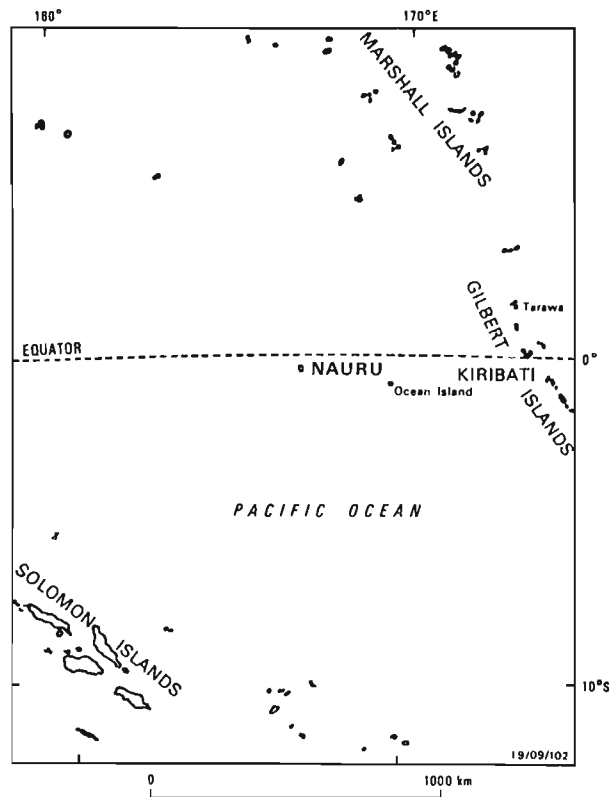


Figure 1. Location of Nauru Island in the Pacific Ocean.

pinnacle surface. Investigations show that about 500 m of Upper Miocene to Quaternary dolomitized limestone cap the seamount. During the hydrogeological investigation the limestone was drilled to a depth of 55 m below sealevel showing intense karstifications to that depth (Jacobson & Hill, 1988, 1993).

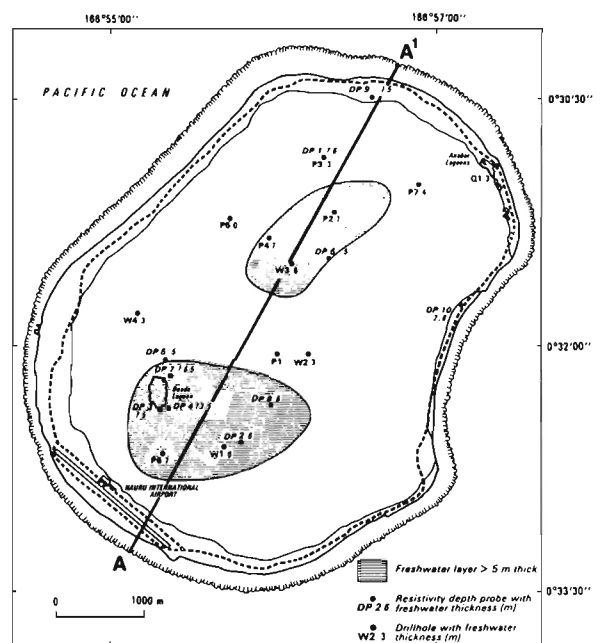


Figure 2. Nauru Island and location of the simulated cross-section A–A1.

The watertable is at an average elevation of 0.3 m above MSL and groundwater flows radially outward to the sea. The island is underlain by a layer of freshwater up to 7 m thick with an average thickness of 4.7 m. Its lower boundary is defined at a salinity level of 1500 mg/L TDS. The freshwater overlies a thick mixing zone of brackish water, which in turn overlies seawater. The average annual rainfall of the island since 1916 is 1994 mm, with a high degree of variability. The maximum record was 4950 mm in 1930, with a minimum 280 mm in 1950. The recharge is about 798 mm, the remaining 1196 mm constituting evapotranspiration (Jacobson & Hill, 1988, 1993). These estimates are based on a probable recharge/rainfall ratio of 40% and, disregarding some groundwater discharge to the sea and the surface water evaporation from lagoons. Therefore, some degree of uncertainty is associated with these estimates. Moreover, recharge is assumed to be uniform throughout the island, although it is probably greater beneath the mined out areas and the lagoons. The present water consumption is estimated to be about 1300 m<sup>3</sup>/d derived from the following sources: rainwater catchment (700 m<sup>3</sup>/d), imported water by phosphate ships (400 m<sup>3</sup>/d), and groundwater from coastal terrace wells (200 m<sup>3</sup>/d).

## Simulation of Nauru aquifer

### 2D Simulation with the "SUTRA" model

To simulate the Nauru aquifer using the SUTRA model, a vertical cross-section of the aquifer along the line A-A<sup>1</sup> (Fig. 2) was considered (Ghassemi & others, 1990). The cross-section is 6400 m long and 120 m deep with an arbitrary thickness of 1 m. It was discretised to 832 rectangular elements and 891 (27 x 33) nodes. The horizontal spacing was constant at 200 m, while the vertical spacing was variable from 2 m to 10 m from the top of the aquifer to a depth of 120 m (Fig. 3). The model was calibrated with the following set of data: hydraulic conductivity (900 m/d), anisotropy (50), recharge (540 mm/yr which is lower than the estimated 798 mm/yr), porosity (30%), longitudinal and transverse dispersivities (65 m and 0.15 m, respectively) and molecular diffusivity (10<sup>-10</sup> m<sup>2</sup>/s). Figure 4 shows some of the results of the calibration.

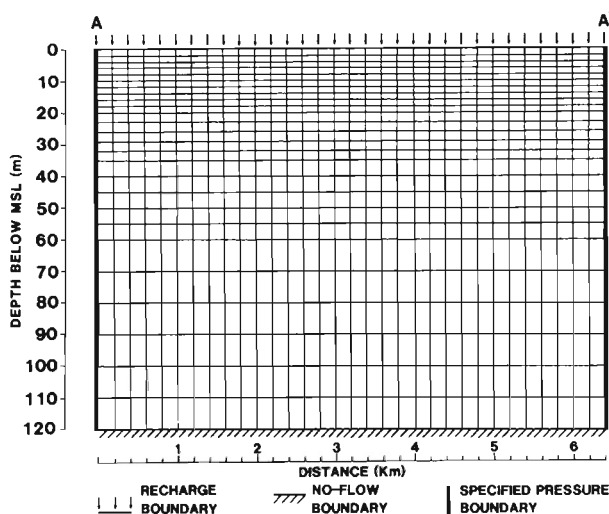


Figure 3. Mesh and boundary conditions.

The calibrated model was used to simulate a number of management options in terms of pumping rates, pumping depths and their locations. One of the simulated options indicated that the simultaneous pumping in five bores, at equal distance of about 1000 m along the cross-section A-A<sup>1</sup>, would have reciprocal effects on each other. These would appear after 3½ years of continuous pumping at a rate of 2.5L/s per bore. This would increase the salinities above the level computed for operation of individual bores. The simulations showed clearly the limitations of simulating a 3D problem with a 2D model. The major limitations were: inability to consider the real boundary conditions of the problem; and difficulties in estimating an appropriate simulated pumping rate based on an estimated radius of influence of the pumping bore and its portion which remains within the simulated slice of the aquifer.

### 3D simulation with the "HST3D" model

In attempts to overcome the limitations of the two-dimensional simulation, the potential of the HST3D model was explored in three stages. Firstly, HST3D was applied in 2D mode to the Nauru Island aquifer employing the same spatial and temporal discretisation as for SUTRA. This caused a major increase in the computed salinities at the centre of the cross-section. To overcome this problem it was required to reduce gradually the horizontal grid size, from 200 m to 2 m toward the centre of the cross-section, and to use short-time steps of one day instead of the 30 day time step used by SUTRA. This increased the computation time significantly.

In the second stage, a small test aquifer, 700 x 700 m and 40 m deep, was designed with a grid size of 100 m in the X-Y directions. The vertical discretisation was set at 3, 6, 10, 15, 22, 30 and 40 m. The parameters were set identical to those estimated by SUTRA for the Nauru aquifer. A bore pumping rate of 5 L/s was applied. The results were generally reasonable.

Finally, the Nauru aquifer was discretised at about 17 000 nodes employing a uniform grid of 200 x 200 m in the X-Y directions (Fig. 5) and a variable one in the vertical direction (2 m from the top to 20 m depth, 3 m from 20 to 35 m, 5 m from 35 to 60 m, and 10 m from 60 to 100 m). CPU time was about 9 minutes per time step on the Australian National University supercomputer Fujitsu VP2200. In another attempt, the number of nodes was reduced to about 12 000 by reducing the simulation depth from 100 to 70 m and changing the vertical discretisation (2 m from the top to 10 m depth, 3 m from 10 to 25 m, 5 m from 25 to 40 m and 10 m from 40 to 70 m). Subsequently, CPU time was reduced to about 4 minutes per time step. The code was subsequently vectorised and the equation solver was substituted with a much more efficient subroutine available on the system. This reduced the CPU time to 5 seconds per time step.

The model required a simulation period of more than 5000 days with short time steps of 0.5 to 1 day to reach steady-state under the influence of its boundary conditions. As the computation time was long and exceeded 8 hours CPU time, the model was run a few times and the computed salinity and pressures used as initial conditions for the subsequent runs, altering the code accordingly. For these runs, the simulation depth was reduced again from 70 to 40 m generating 10 000 nodes and requiring a CPU time of about 3.5 seconds per time step.

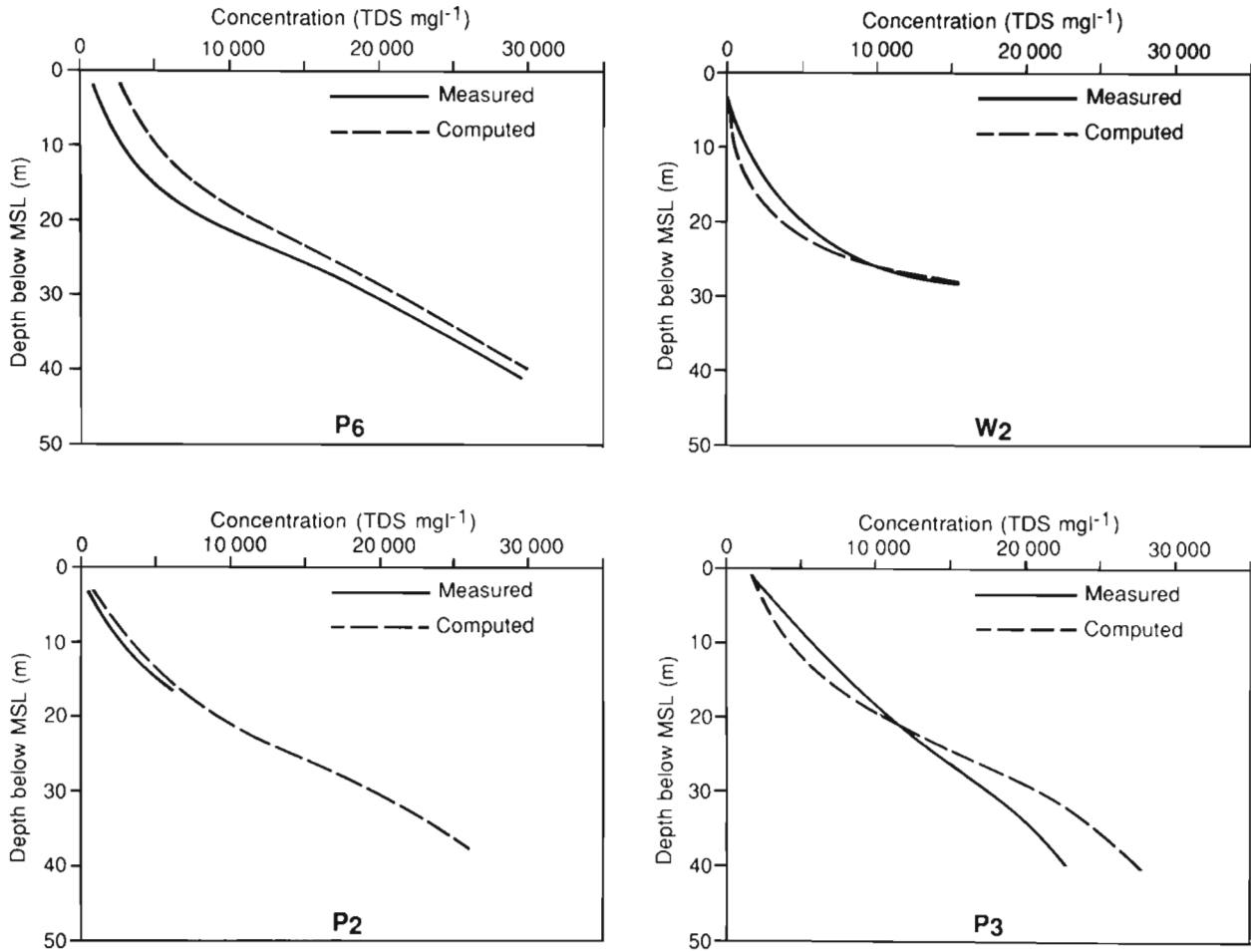


Figure 4. Measured and computed (with SUTRA) groundwater salinity values at four observation bores.

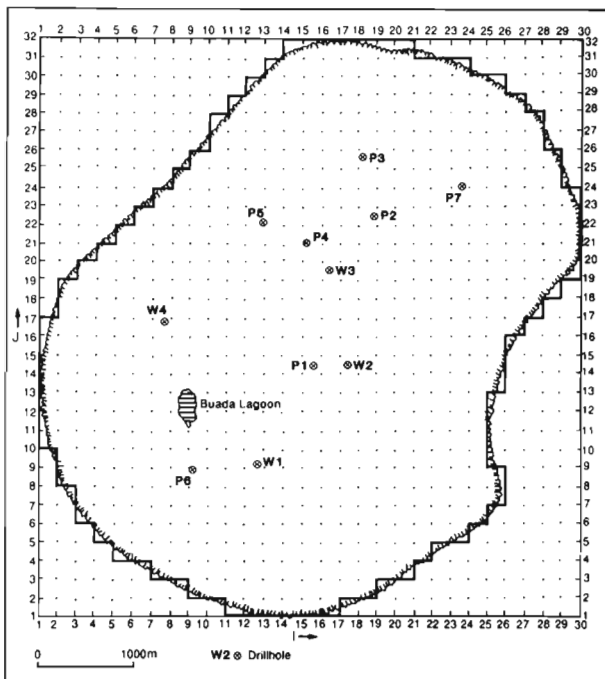


Figure 5. Discretisation of the Nauru aquifer.

The model was calibrated with the following parameters: a hydraulic conductivity of 700 m/d; and recharge rate of 750 mm/yr over the major part of the island with the exception of the area surrounding the Buada Lagoon, which is located in a depression and has a higher thickness of freshwater. This area was simulated with a higher recharge rate of 850 mm/yr. The other parameters were the same as those simulated by SUTRA. While the hydraulic conductivity is 200 m/d lower than in the case of the SUTRA model calibration, recharge rates are higher and much closer to the estimated value of 798 mm for the island. Figure 6 shows the results of the calibration and compares the measured and the computed values in four observation bores. As Figure 6 shows, computed salinities do not match the measured values closely. This is owing to the lack of spatial distribution of basic parameters, such as hydraulic conductivity, porosity, anisotropy, and the recharge rate.

Figure 7 shows three vertical cross-sections of the computed salinities, indicating clearly the extent of the transition zone between the fresh and saline seawater. Figure 8 shows computed salinity contours at a depth of 2 m. Generally, it shows the gradual decrease of salinities towards the centre of the aquifer. However, it should be noted that the salinity contour lines of 1500, and 1000 within the larger contour line of 1000 mg/L, are reflections of the cusp created by the model.

The sensitivity of computed salinities to major parameters (hydraulic conductivity, recharge rate and dispersivity)

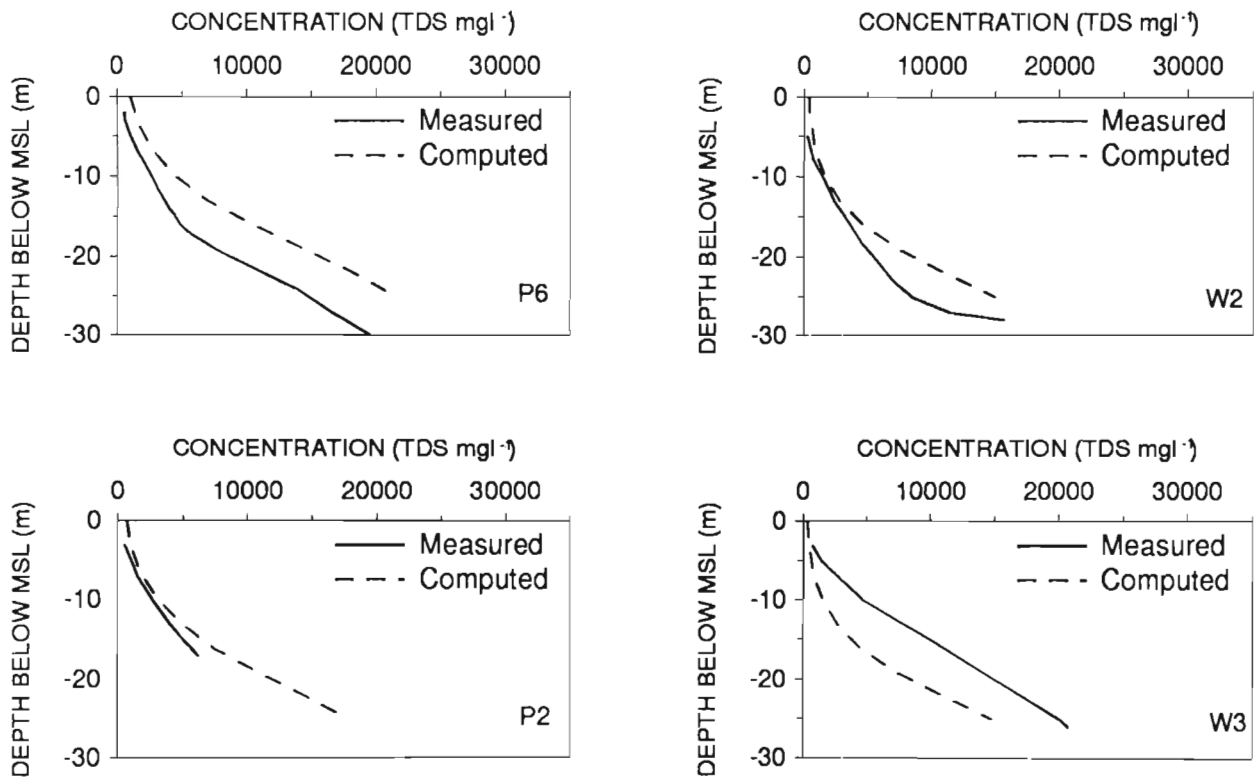


Figure 6. Measured and computed (with HST3D) salinity values at four observation bores.

was analysed. Tables 1 to 3 compare salinity values of the calibrated model with those computed during the sensitivity analysis at eight nodes on the cross-section J=16 and columns 5, 10, 15 and 20 (Fig. 8) at depths of 2 m and 4 m. Table 1 shows that the increase of the hydraulic conductivity from 700 to 800 m/d increases the computed salinity values. Table 2 indicates that reduction of the recharge rate increases the computed salinities, while Table 3 shows that reduction of the dispersivity values decreases the salinities.

Following the process of model calibration and sensitivity analysis, the calibrated model was used to simulate the effect of pumping at simulated wells A, B, C, D at a depth of 2 m with pumping rates of 1, 2 and 4 L/s. Figure 9 shows that pumping at a rate of 1 L/s at site A and at a depth of 2 m does not encourage seawater intrusion and upconing of saline water under the pumping sites. This is due to the pumping rate being less than the recharge rate of 850 mm per year (1.08 L/s) around the Buada Lagoon, and is almost equal to the recharge rate of 750 mm per year (0.95 L/s) over the remainder of the aquifer. Pumping at higher rates of 2 and 4 L/s causes significant rise in groundwater salinity and upconing of seawater near pumping sites. These results show that in similar environments, in order to prevent any increase in aquifer salinity, the abstraction rate should not exceed the recharge rate. Figure 10 shows the effects of pumping at rate of 1 to 4 L/s and at a depth of 2 m, at the simulated wells A, B, C and D (Fig. 8) over a period of 1250 days. It indicates that a new steady-state salinity regime will be established after about 300 days.

## Conclusions

SUTRA is a powerful tool for the simulation of density dependent solute transport in porous media. However, its application should be restricted to two-dimensional prob-

lems. Simulation of complex three-dimensional problems with SUTRA could lead to erroneous parameter estimation, model calibration and thus subsequently wrong conclusions.

Three-dimensional discretisation of Nauru Island aquifer and simulation with the HST3D model had the major advantage of being able to specify natural boundary conditions as well as the stresses. However, this required access to supercomputing facilities. The HST3D model computation also required short time steps of 0.5 to 1 day to produce reasonable results. Even with such short time steps it produced a cusp at the centre of the aquifer because of the grid size of 200 x 200 m. Overcoming this problem would require a finer discretisation and a concomitant increase in the number of nodes and computation time. Other observations with respect to the simulation of Nauru aquifer with HST3D model are as follows:

- Nauru aquifer consists of an intensely karstic limestone. Its three-dimensional simulation requires a reasonable knowledge of the major parameters, mainly hydraulic conductivity, recharge rate, porosity and anisotropy. However, as these parameters were unavailable the model was calibrated with a uniform distribution of each parameter (even the value of these parameters were unavailable and an estimated value based on similar cases was adopted). The exception was the recharge rate, where two recharge zones were considered. This lack of data has affected the calibration result.
- Although the results of calibration with HST3D are not as impressive as with SUTRA, the simulated recharge rates with HST3D are much closer to estimated values for the island.
- HSTSD was sensitive to changes in grid size in the

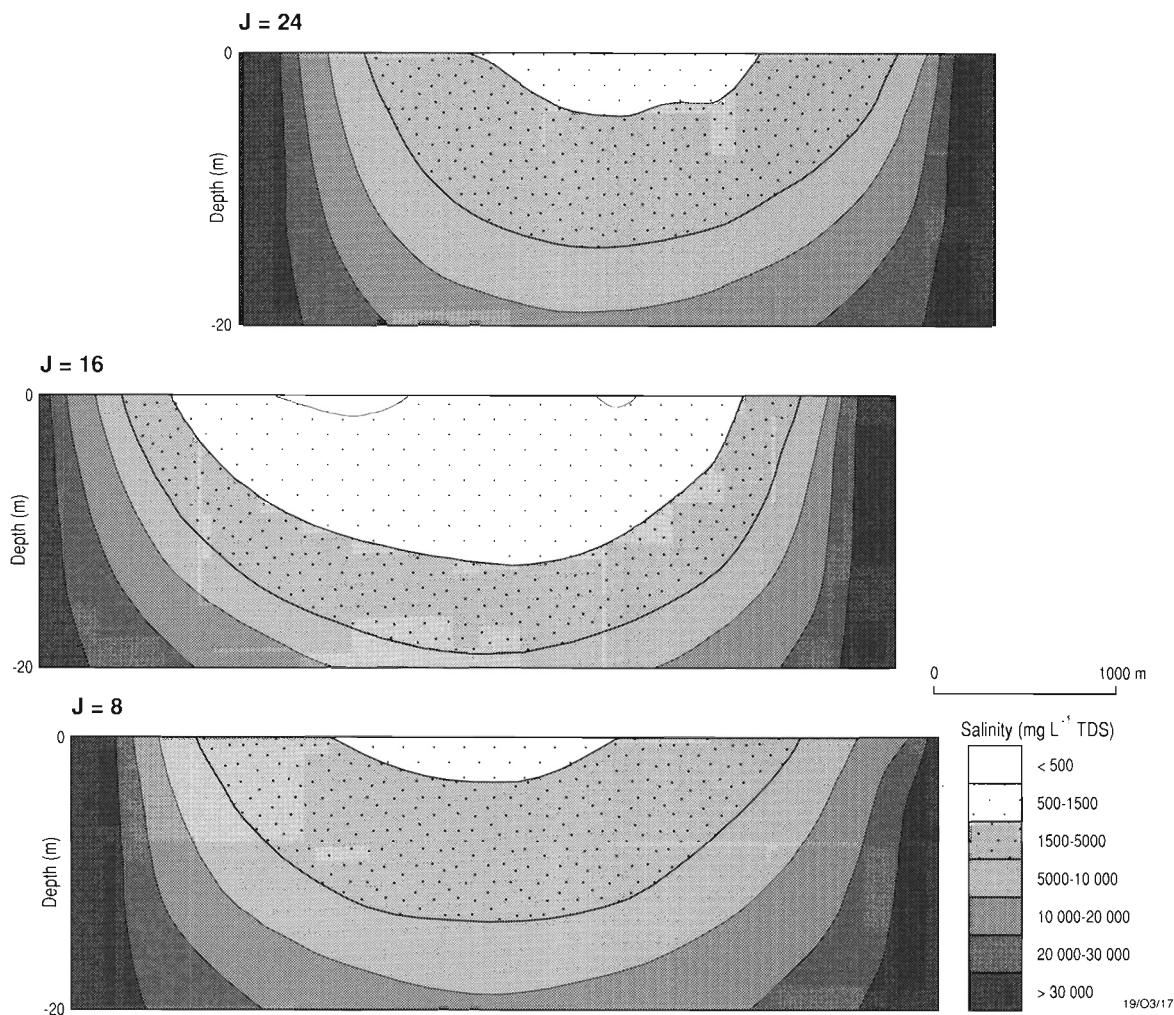


Figure 7. Cross-section of computed salinities (in mg/L TDS) along the lines J=8, J=16 and J=24 (see Figure 5) from sealevel to a depth of 20 m.

vertical direction. A more uniform vertical grid size compatible with the horizontal grid size would produce better results. However, this was not possible to implement because of the constraints on computational time.

Overall, it can be concluded that where requisite data and adequate computing facilities are available, the HST3D model is suitable for three-dimensional simulation of seawater intrusion. The use of supercomputing facilities becomes inevitable, if the problem is not a small-scale one.

### Acknowledgements

The author thanks K.L. Kipp for his advice during this exercise, and W.R. Evans and I. Acworth for their useful comments on the original manuscript. The computations upon which this work is based were carried out using the Fujitsu VP2200 supercomputer at the Australian National University. In this respect, we are grateful to the management of the Supercomputer Facility. We also thank Heather Symons for her early computational work, and Susan Kelo for word processing.

### References

- Falkland, A. (editor), 1991 — Hydrology and Water Resources of Small Islands: A Practical Guide. Paris: UNESCO pp 435.
- Ghassemi, F., Jakeman, A.J. & Jacobson, G., 1990 — Mathematical modelling of sea water intrusion, Nauru Island. *Hydrological Processes*, 4(3), 269–281.
- Jacobson, G. & Hill, P.J., 1988 — Hydrogeology and groundwater resources of Nauru Island, Central Pacific Ocean. *Bureau of Mineral Resources, Geology and Geophysics, Canberra, Record* 1988/12, pp 87.
- Jacobson, G. & Hill, P.J., 1993 — Groundwater and the rehabilitation of Nauru. In McNally, G., Knight, M. & Smith, R. (editors), *Collected Case Studies in Engineering Geology, Hydrogeology and Environmental Geology. Butterfly Books, Sydney*, 103–119.
- Kipp, K.L., 1987 — HST3D: A Computer Code for Simulation of Heat and Solute Transport in Three Dimensional Ground-Water Flow Systems. *US Geological Survey. Water Resources Investigations, Report* 86-4095, pp 517.
- Reilly, T.E. & Goodman, A.S., 1985 — Quantitative analysis of saltwater freshwater relationships in groundwater systems — a historical perspective. *Journal of Hydrology*, 80, 125–160.

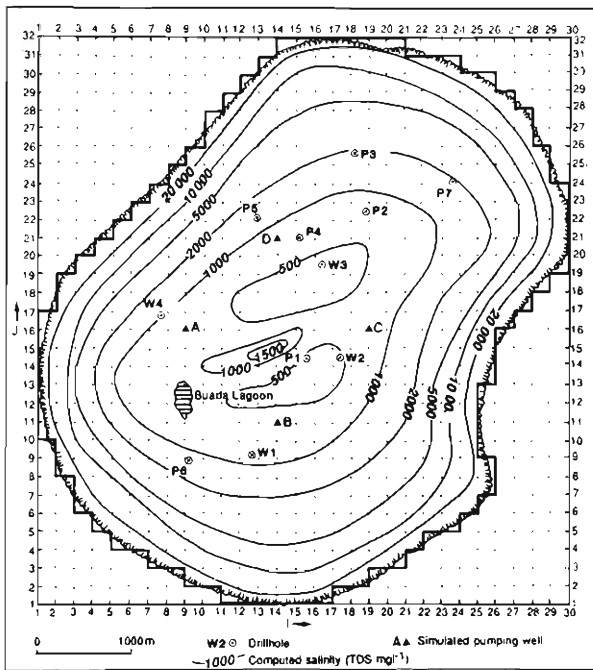


Figure 8. Computed salinity contour lines at a depth of 2 m.

Reilly, T.E. & Goodman, A.S., 1987 — Analysis of saltwater upconing beneath a pumping wells. *Journal of Hydrology*, 89, 169–204.

Voss, C.I., 1984 — SUTRA, Saturated–Unsaturated TRAsport: A Finite-Element Simulation Model for Saturated–Unsaturated Fluid–Density–Dependent Groundwater Flow with Energy Transport or Chemically Reactive Single-Species Solute Transport. *US Geological Survey. Water Resources Investigations, Report 84-4369*, pp 409.

Table 1. Sensitivity of computed salinities (in mg/L TDS) with respect to change in hydraulic conductivity at 8 nodes on the cross-section J=16 (see Fig. 8).

Hydraulic conductivity (m/d)	Depth (m)	Column no. (I)				Remarks
		5	10	15	20	
700	2	2030	550	1090	880	calibrated model
700	4	2940	740	1160	1116	calibrated model
800	2	2320	540	930	920	sensitivity analysis
800	4	3360	730	1000	1210	sensitivity analysis

Table 2. Sensitivity of computed salinities (in mg l<sup>-1</sup> TDS) with respect to change in recharge rate at 8 nodes on the cross-section J=16 (See Fig. 8).

Annual recharge (mm)	Depth (m)	Column no. (I)				Remarks
		5	10	15	20	
750–850	2	2030	550	1090	880	calibrated model
750–850	4	2940	740	1160	1116	calibrated model
650–750	2	2360	550	950	940	sensitivity analysis
650–750	4	3420	570	1030	1240	sensitivity analysis

Table 3. Sensitivity of computed salinities (in mg l<sup>-1</sup> TDS) with respect to change in longitudinal ( $\alpha_L$ ) and transversal ( $\alpha_T$ ) dispersivities at 8 nodes on the cross-section J=16 (see Fig. 8).

$\alpha_L$ (m)	$\alpha_T$ (m)	Depth (m)	Column no. (I)				Remarks
			5	10	15	20	
65	0.15	2	2030	550	1090	880	calibrated model
65	0.15	4	2940	740	1160	1116	calibrated model
52	0.12	2	1540	440	980	690	sensitivity analysis
52	0.12	4	2400	620	1050	950	sensitivity analysis

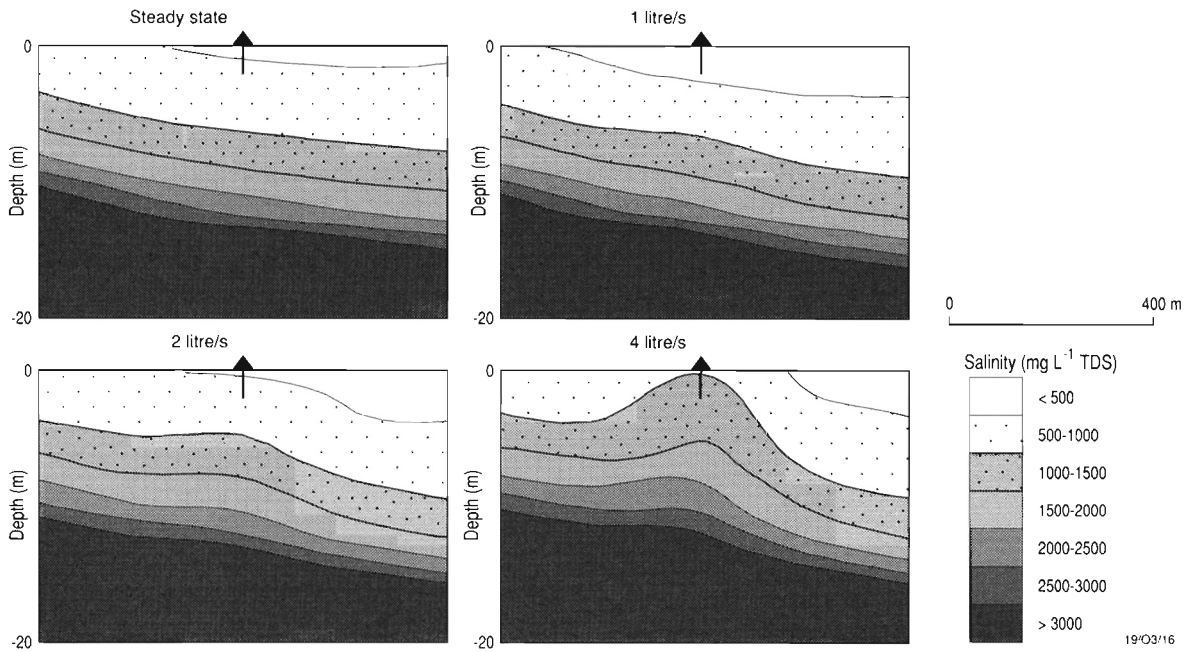


Figure 9. Effect of pumping at the simulated well A with three different pumping rates in cross-sections of 20 m depth and 800 m width (salinities in mg/L TDS).

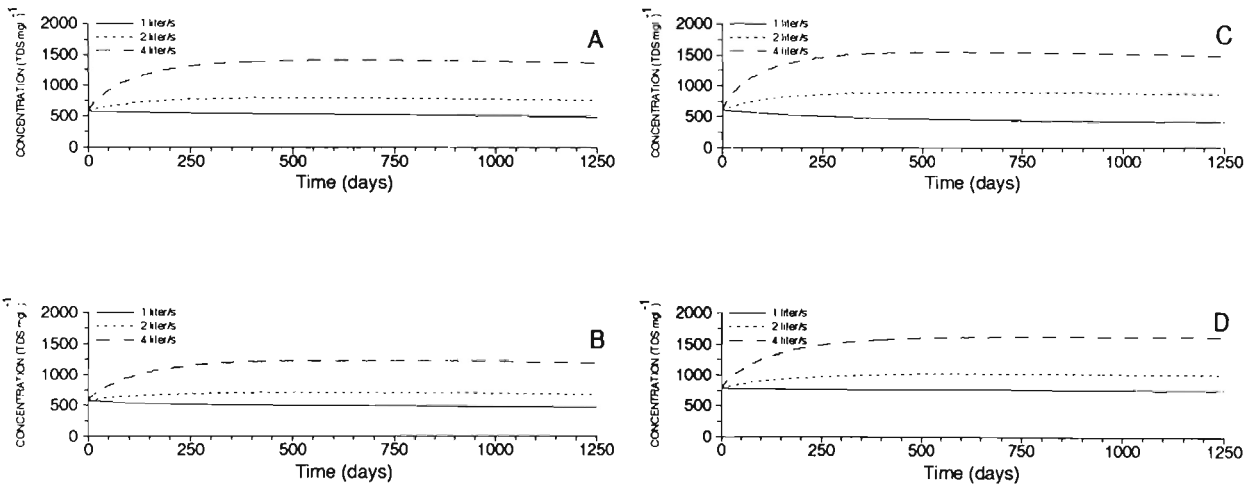


Figure 10. Effects of pumping at simulated wells, A, B, C, and D over a period of 1250 days.